



Published in final edited form as:

*Mol Ther.* 2006 June ; 13(6): 1163–1172.

## Nonviral Gene Delivery from Nonwoven Fibrous Scaffolds Fabricated by Interfacial Complexation of Polyelectrolytes

Shawn H. Lim, I-Chien Liao, and Kam W. Leong\*

Department of Biomedical Engineering, Johns Hopkins University School of Medicine, 720 Rutland Avenue, 729 Ross Research Building, Baltimore, MD 21205, USA

### Abstract

We investigated a novel nonwoven fibrous scaffold as a vehicle for delivery of DNA. Fibers were formed by polyelectrolyte complexation of water-soluble chitin and alginate, and PEI–DNA nanoparticles were encapsulated during the fiber drawing process. Nanoparticles released from the fibers over time retained their bioactivity and successfully transfected cells seeded on the scaffold in a sustained manner. Transgene expression in HEK293 cells and human dermal fibroblasts seeded on the transfecting scaffolds was significant even after 2 weeks of culture compared to 3-day expression in two-dimensional controls. Fibroblasts seeded on scaffolds containing DNA encoding basic fibroblast growth factor (bFGF) demonstrated prolonged secretion of bFGF at levels significantly higher than baseline. This work establishes the potential of this fibrous scaffold as a matrix capable of delivering genes to direct and support cellular development in tissue engineering.

### Keywords

tissue engineering; fibrous scaffold; nonviral gene delivery; polyelectrolyte; cell therapy

### Introduction

Gene therapy may augment cell therapy, which in turn may be facilitated by the application of tissue engineering concepts to affect cell behavior. Release of bioactive factors entrapped within three-dimensional polymeric scaffolds has been shown to stimulate and direct cellular processes that promote cell adhesion, proliferation, and/or differentiation and tissue integration [1–3]. However, loss of bioactivity of the growth factors due to encapsulation [4], low incorporation efficiencies [5], and high burst release kinetics [6] has dampened the effectiveness of this approach. Also, some biological signals such as intracellular signaling molecules or transcription factors cannot be applied as soluble factors. An attractive alternative to protein delivery is to entrap DNA that encodes such therapeutic proteins within the polymeric scaffold. The released gene vectors will then transfect the seeded cells to produce the gene products or biological signals locally and in a sustained manner.

Several polymeric materials have been previously investigated as DNA delivery systems. *In vivo* implantation of various collagen-based and poly(lactide-co-glycolide) DNA-containing matrices in wound-healing paradigms showed improved tissue integration [7–10]. Despite these promising results, several challenges remain to be addressed in the development of scaffold-based gene delivery. Encapsulation of naked plasmid DNA limits the scope of these therapies as very high amounts of DNA must be delivered to elicit a physiological response. Additionally, DNA-delivering scaffolds that have been investigated to date are unable to

---

\*To whom correspondence and reprint requests should be addressed. Fax: +1 443 287 3099. E-mail: kleong@bme.jhu.edu.

present gene vectors in a spatially defined manner. This would be useful for engineering multicellular tissue constructs, which would require localization of cell signals. The use of fibrous scaffolds for this application presents a distinct advantage over such conventional scaffolds as they possess the potential for spatial organization via textile engineering methods such as microbraiding or employing single fibers as individual structural units [11].

Much research has been done on the application of chitosan [12–16] and alginate [17–19], two naturally derived polysaccharides, as biomaterials for tissue engineering and drug delivery. In aqueous form, molecules of chitosan and alginate assume a net positive and negative charge, respectively. Complex formation via charge neutralization of mixtures of these two polyelectrolytes can be exploited as a means of facile, mild preparation of a novel polymeric scaffold [20–22]. This principle of polyelectrolyte complexation can be extended to the formation of a self-assembled fiber as a structural building block for scaffold construction [23,24]. Fibers consisting of a complex of chitin and alginate can be drawn from an interface between the two polyelectrolyte solutions. The continuous removal of newly formed complex encourages further diffusion of polyions toward the interface, allowing uninterrupted fiber formation. More importantly, because of the aqueous conditions and low temperatures involved, biologically active materials such as drugs, proteins, and genes can be easily incorporated into the fibers without the risk of significant loss of function [11,25].

We propose to create transfecting scaffolds capable of continuous gene delivery by encapsulating DNA nanoparticles within the fibers. Polyethylenimine (PEI)–DNA nanoparticles released from the fibers can transfect cells seeded within the scaffold, thus directing the production of factors in a temporally defined manner. Chitin–alginate polyelectrolyte fibers are ideally suited to this application because the mild complexation conditions, combined with high encapsulation efficiency, contribute to maintaining the potency of encapsulated DNA. We demonstrate that uptake of these DNA complexes by cells can lead to prolonged and effective transgene expression.

## Results

### Production of Nonwoven Fibrous Scaffold and Encapsulation of PEI–DNA Nanoparticles

We employed fibers comprising a self-assembled polyelectrolyte complex of water-soluble chitin (WSC) and alginate with encapsulated PEI–DNA nanoparticles as the structural basis for the fabrication of a novel transfecting three-dimensional tissue engineering scaffold. Fiber formation was initiated by bringing into contact a small quantity of a solution of each polyelectrolyte, forming a complex via charge neutralization. The complex in the form of a fiber was drawn upward with mechanical rotors and then allowed to air-dry. Fibers had two distinct regions—a continuous fiber region, approximately 10–20  $\mu\text{m}$  in diameter, as well as evenly distributed swellings along its length—a so-called “bead” region—that was several times larger (Figs. 1A and 1B). (Under certain processing conditions, it was also possible to produce fibers that lacked this bead region, but we did not investigate this in this study.) Once dried, fibers were easily collected and processed into a nonwoven three-dimensional fibrous scaffold using a textile engineering technique known as needle-punching. A macroscopic view of the scaffold suggests that it possesses high porosity, a characteristic that was confirmed by imaging with scanning electron microscopy (Fig. 1C). Random entanglements between fibers provide the physical reinforcement that holds the scaffold together, and the pores between fibers are on the order of tens of micrometers in diameter. There was no visible difference between fibrous scaffolds containing the PEI–DNA nanoparticles and blank fiber scaffolds.

We successfully encapsulated PEI–DNA nanoparticles into WSC–alginate fibers formed by polyelectrolyte complexation. To achieve this, we mixed the solution of nanoparticles with the solution of water-soluble chitin prior to the fiber drawing process. Mixing the nanoparticles,

which have a positive  $\zeta$  potential, with the positively charged WSC prevented their premature aggregation around alginate molecules. This avoided precipitation of alginate, which would hinder fiber formation. Imaging of the individual fibers using phase and confocal microscopy confirmed the presence and distribution of the fluorescently stained nanoparticles within a single fiber as well as in the scaffold (Fig. 2). We observed nonaggregated nanoparticles distributed throughout the fibers in a random fashion, with a sparser distribution of particles in the bead region of the fiber compared with the core fiber section. The density distribution of particles within the bead region also suggested that the axis of the bead has a higher concentration of polyelectrolyte complex and thus was denser than the surrounding material. The bead formation is likely an artifact resulting from the fiber drawing process, in which the rate of fiber drawing exceeds the optimal rate of complexation between the polyelectrolytes.

### Cell Seeding and Viability on Fibrous Scaffolds

The scaffold swelled visibly and decreased in opacity after it was immersed in cell medium, while still retaining its fibrous morphology (Fig. 3A). This was most likely due to the absorption of water into the bead regions of the fibers by residual free charges due to incomplete neutralization in a nonstoichiometric mixture of polyelectrolytes. Approximately 30% of the initial number of human epithelial kidney (HEK293) and human dermal fibroblast (HDF) cells seeded, using a static seeding method attached to the scaffold, with the rest falling through the pores and adhering to the Transwell membrane. Cells remained viable on the scaffold for the entire duration of the experiment as confirmed by the live/dead staining assay (Fig. 3B), although we observed cells to detach occasionally from the fibers and adhere to the bottom of the culture wells.

### Transgene Expression of Green Fluorescent Protein in Cells Seeded on Scaffold

We fabricated fibrous scaffolds loaded with PEI–DNA nanoparticles containing green fluorescent protein (GFP)-encoding plasmid and studied them as a demonstration of the transfectability of cells seeded on the scaffolds. The image in Fig. 4A was acquired using confocal microscopy performed on nanoparticle (NP)–GFP scaffold samples seeded with HEK293 cells 12 days postseeding. We observed active expression of cytoplasmic GFP in a significant number of cells, even at such a late time point. We observed single-cell outlines about 10  $\mu\text{m}$  in diameter, indicating that cells did not aggregate on the scaffold but remained separate. However, cells retained a rounded morphology, in contrast with the spread morphology of these cells when cultured in a two-dimensional configuration. To quantify the extent of transfection, we trypsinized cells from the scaffold and analyzed them using fluorescence-activated cell sorting (FACS; Fig. 4B). Up to 18.5% of cells from the scaffolds in the experimental group were GFP-positive, comparing favorably with about 20% for the positive control, which contained cells that were transfected with LipofectAMINE-complexed plasmid DNA on a tissue-culture polystyrene plate (TCPS). GFP expression was not detected in nontransfected cells from the negative control, confirming no endogenous production of the observed transgene product.

Human dermal fibroblasts seeded on the scaffold had an increased tendency to cluster and form aggregates compared to the HEK293 cells. Regardless, we observed GFP expression uniformly throughout the clusters of cells seeded on NP–GFP scaffolds, indicating that cellular aggregation did not pose a physical barrier to the transport of nanoparticles to the cells (Fig. 5). Flow cytometry analysis of the fibroblasts reported a trend similar to that observed in HEK293 cells, with up to 8% of cells in the sample group exhibiting GFP expression at the 12-day time point, compared with 11% of cells transfected in two-dimensional culture in the positive control group; nontransfected cells did not exhibit any GFP expression. The disparity in the overall gene expression levels in HEK293 and HDF was most likely due to the transfectability of different cell types by PEI–DNA nanoparticles.

It should be noted that recovery of free fibroblasts from the scaffold for analysis was much more difficult than for the HEK293 cells, with fewer cells being recovered in general. Cell harvesting by trypsin digestion from the scaffold samples and removing the supernatant yielded almost no cells; only by physically breaking up the scaffold using vigorous pipetting and vortexing, followed by centrifugation, was it possible to collect a sufficient quantity for analysis.

### **Sustained Production of Therapeutic Cytokine—Basic Fibroblast Growth Factor (bFGF)**

To demonstrate the sustained transfection characteristics, we loaded scaffolds with nanoparticles containing plasmid DNA with the gene encoding bFGF as a model therapeutic cytokine. We sampled the scaffold incubation medium at regular intervals and analyzed the concentration of secreted bFGF in the supernatant over a period of 21 days using enzyme-linked immunosorbent assay (ELISA) and then normalized it to the initial cell number (Fig. 6). Secretion of bFGF from cells seeded on NP–bFGF scaffolds was significantly enhanced over a period of at least 13 days. The concentration of bFGF in medium incubated with NP–bFGF cell-scaffold constructs peaked at 97 pg/ml at 3 days postseeding, decreasing monotonically in a quasilinear manner for 2 weeks, before beginning to level off after 16 days in culture. The baseline used for comparison was the measured concentration of bFGF in media sampled from control blank scaffolds containing no PEI–DNA nanoparticles with fibroblasts seeded on them. Normalized levels of bFGF in the control remained almost constant around 20 pg/ml for the entire time course of the experiment, indicating that the upregulation of bFGF secretion in scaffolds with nanoparticles was effected by the transfection of cells in the scaffolds.

In contrast to transfection from the NP–bFGF scaffolds, fibroblasts transfected in two-dimensional plate culture exhibited increased levels of bFGF secretion for less than a week. A peak value of 74.5 pg/ml per  $10^5$  cells was recorded after 3 days, but this enhancement of bFGF production in transfected fibroblasts was not maintained, and measured concentration dropped sharply to basal levels soon after. Even at the peak concentration, bFGF concentration per cell was notably lower in comparison to that of NP–bFGF scaffolds. This outcome was expected as the cells cultured in two-dimensional culture were given only a bolus delivery of the PEI–DNA nanoparticles. The results reinforce the hypothesis that there is a sustained release of PEI–DNA nanoparticles from the fibrous scaffolds, leading to a prolonged transfection of cells and thus continuous secretion of the transgenic product.

A further comparison of the experimental end-point concentrations of bFGF yielded some interesting observations. Fig. 7 presents the measured concentrations at the final time point in each experimental condition, without normalizing the levels to cell number. A level of 9.2 pg/ml bFGF was detected in fresh serum-containing medium used to culture the fibroblasts; this was used as the threshold level of sensitivity of the assay. Medium incubated with HDF cells seeded on blank scaffolds exhibited a low endogenous level of bFGF that was significantly higher than in fresh medium alone. This endogenous concentration was also observed to coincide with the leveling-off of bFGF in medium samples that had been incubated with transfected cells on the NP–bFGF scaffolds. Conversely, fibroblasts cultured on TCPS did not result in an elevated extracellular bFGF concentration, regardless of whether they had been previously transfected with PEI–DNA nanoparticles. The results demonstrate that in plate culture, fibroblasts do not normally secrete bFGF, but when cultured in a three-dimensional configuration, upregulation of bFGF production follows without induction by a transgene.

To appreciate fully the impact of the transfecting fibrous scaffold, it was necessary to address an additional concern as to the instability of secreted bFGF in the medium. To investigate this, we added 200 pg/ml soluble bFGF to fibroblast medium and incubated it for 1 and 3 days; after this time we sampled the medium and assayed it to determine the concentration of bFGF

remaining. Since ELISA is a highly specific protein assay, denatured growth factor would not contribute to the measured level. The results indicate that the stability of extracellular bFGF in serum-containing fibroblast medium was extremely low, with only about 10% of the initial amount recoverable after 1 day of incubation and less than 5% recoverable after 3 days. In fact, more than 15% of the bFGF denatured immediately upon addition to cell medium. This strongly suggests that transfected cells on the scaffold secreted a greater amount of bFGF than was actually detected, and the data obtained were in fact an underestimate of the efficiency of transfection of fibroblasts by the nanoparticles released from the fibers. This finding, combined with the end-point analysis, lends support to our conclusion that fibroblasts in three-dimensional culture secrete bFGF in an endogenous fashion.

## Discussion

WSC–alginate fibers were formed by initiation of complex formation followed by a continuous upward drawing motion using mechanical rotors. As this complex was drawn upward, depletion of the interface caused the inward diffusion of free polyelectrolyte molecules; gene vectors were likewise pulled inward and encapsulated within the polyelectrolyte-complexed (PEC) fibers. These PEC fiber scaffolds pose an attractive alternative to the other types of scaffold-based gene delivery systems as they possess high porosity and employ a fabrication process that is capable of encapsulating gene vectors without the use of chemical linkers. This is unique as the gene vector is incorporated directly within the structural unit of the fiber itself. Despite concerns about the toxicity of PEI–DNA complexes [26], no adverse effect on cell viability was observed, as the sustained release of the complexes would not overwhelm the cells, unlike a high-concentration bolus dose in a typical transfection protocol.

In this model of transfection from a three-dimensional scaffold, PEI–DNA nanoparticles released from the fibers over time would be continuously taken up by the cells. The percentage of cells seeded on NP–GFP scaffolds expressing GFP after 2 weeks was comparable to the early expression in cells transfected in two-dimensional culture using a commercially available nonviral transfection reagent. A previous study of the kinetics of GFP expression in transfected cells demonstrated that fluorescence was highly transient, peaking 24 h after transfection but decreasing to undetectable levels within 96 h [27]. The dominant factor responsible for this observation was most likely from dilution of the signal due to cell proliferation. Taken together with our observations, it can reasonably be concluded that nanoparticles were continuously released; thus GFP expression by transfected cells could be achieved over a more sustained period compared to a one-time delivery of the gene vector.

Basic fibroblast growth factor is a powerful mitogen implicated in cell proliferation and angiogenesis [28]. However, therapeutic delivery of bFGF in its bioactive form is a challenge due to its rapid degradation kinetics [29]. Sustained delivery of the bFGF gene is desirable as it ensures that it will be manufactured and secreted in the proper conformation. Cells seeded on NP–bFGF scaffolds had prolonged secretion of bFGF up to 2 weeks at levels significantly higher than baseline, while transfection of cells grown in two-dimensional culture demonstrated that production of bFGF by bolus-transfected HDF cells could not be sustained in the long term. These observations reiterate the previous conclusion that the release of nanoparticles from the fibrous scaffolds occurred over an extended time scale.

In addition to the continuous release of gene vectors, other factors are hypothesized to contribute to the prolonged gene expression in cells within the fibrous scaffolds. Using the PEC fibers as a source of nanoparticles enhances their bioavailability as they are released from these fibers directly into the cellular microenvironment of the seeded cells. The local concentration of vectors is elevated, thus increasing the overall percentage of cells that are exposed to, and subsequently uptake, the vectors [30]. Maintaining cells in a three-dimensional

configuration could also be a mediating factor in enhancing transfection and gene expression. Xie and colleagues have postulated that the three-dimensional environment allows for enhanced transmission of biochemical and mechanical signals between cells, potentially resulting in increased uptake of gene vectors as well as prolonged transgene expression [31]. A study of the molecular composition of cell adhesion demonstrated that two-dimensional plate culture induces an artificial polarity between the upper and the lower surfaces of normally nonpolar cells, resulting in the formation of adhesive structures that differ drastically from that observed in three-dimensional culture [32]. It can be reasoned that there is unequal efficiency of vector uptake from the top and bottom sides of cells in plate culture, an inequity that can be resolved by transfecting cells on three-dimensional scaffolds. In addition, the sustained release of gene vector ensures its constant availability over several complete cycles of cell proliferation, including over the mitotic stage of the cell cycle during which cells exhibit the highest transfection efficiency [33].

The scaffold-based gene delivery system presented in this work utilized PEI–DNA nanoparticles as a model nonviral gene vector. PEI–DNA nanoparticles encapsulated within implantable three-dimensional poly(lactide-co-glycolide) scaffolds have been studied by Huang *et al.* [34] and shown to be an efficient means to deliver DNA to infiltrating cells *in vivo* [10,35]. However, the process of polyelectrolyte complexation presented here can potentially be employed as a means of encapsulation and controlled release of a far wider range of gene vectors, including but not limited to other forms of nanoparticles, microparticles, and even viral vectors. We have previously demonstrated that cells, including endothelial and mesenchymal stem cells, can be encapsulated in this type of scaffold and maintain their viability for at least 6 weeks [11]. At this time, the mechanism and kinetics of release of nanoparticles from the fibers remain to be elucidated; however, they are believed to be largely diffusion-dependent. Incomplete charge neutralization between the amino group on WSC and carboxyl group on alginate molecules during complexation results in residual positive and negative charges, respectively. These charges are free to interact electrostatically with charged particulates in solution—for example, the net-positive PEI–DNA nanoparticles—and retain them within the fibers. Over time, the influence of interactions with ions in the culture medium, combined with the degradation of the fibers, allows the nanoparticles to escape. Such a fibrous scaffold can be used as a complementary technology to deliver gene vectors tailored for specific cell types, for example, containing conjugated cell- or nuclear-targeting ligands. In all instances, it would be necessary to optimize the rate and profile of release of these vectors, which could conceivably be achieved by altering the relative charge densities within the fiber by changing the initial polyelectrolyte concentration or by using different combinations of polyelectrolytes. The simplicity and versatility of the complexation process make the fibrous scaffold a powerful technology for controlled delivery of genes that can mediate and direct cellular development within a tissue-engineered construct.

## Experimental Methods

### Materials

Crab shell chitin, polyethylenimine (branched, 25 kDa), and low-viscosity alginic acid (60/40 mannuronic acid/guluronic acid) were purchased from Sigma (St. Louis, MO, USA). Prior to use, the chitin was modified in a homogeneous deacetylation process using sodium hydroxide [36] to obtain WSC. The final product was washed several times in a mixture of acetone and water and then freeze-dried, resulting in a brownish-yellow loose precipitate. After modification, the degree of deacetylation was determined to be approximately 51% using first-derivative UV spectroscopy [37] in a Shimadzu UV-160 spectrophotometer. The fluorescent protein reporter gene used was pEGFP-C1, a 4.7-kb pcDNA encoding GFP, driven by a cytomegalovirus (CMV) immediate early promoter (Clontech, Palo Alto, CA, USA). Plasmid

encoding basic fibroblast growth factor (pVR1055-bFGF) was created by excising the bFGF gene from the pVIVO-bFGF plasmid (InvivoGen, San Diego, CA, USA) and then ligating it into the CMV-driven blank vector pVR1055, which is the backbone of the pVR1255 plasmid encoding firefly luciferase (kindly provided by Dr. Carl Wheeler, Vical, Inc.). The pVR1055-bFGF was expanded from transformed DH5 $\alpha$  cultures and purified using a Qiafilter Plasmid Giga Kit (Qiagen, Valencia, CA, USA).

### DNA nanoparticles

PEI–DNA nanoparticles were synthesized at a nitrogen/phosphate ratio of 10/1 in a 5% sterile glucose solution [38]. Briefly, 3  $\mu$ l of 100 mM PEI solution in 50  $\mu$ l glucose solution was pipetted into 10  $\mu$ g of plasmid DNA in 50  $\mu$ l glucose solution, vortexed for 30 s, and allowed to stand at room temperature for 15 min. Nanoparticles were characterized in a Zetasizer (Malvern Instruments) and found to have a  $\zeta$  potential of  $29 \pm 4$  mV, with an average diameter of 130 nm.

### Scaffold fabrication

Solutions of 0.75% WSC and 1% alginate were prepared by dissolving each in distilled water. A 10- $\mu$ l droplet of each solution was deposited in contact with each other on the surface of a tissue-culture plate, and a single fiber was drawn vertically from the interface of the two solutions at a rate of 10 mm/s using speed-controlled mechanical rollers and allowed to air-dry. Multiple fibers can be drawn simultaneously with this system, culminating in the formation of a bundle of dry fibers. PEI–DNA nanoparticle-loaded fibers were produced by adding a solution of the nanoparticles (20  $\mu$ g DNA per milliliter of WSC solution, estimated from the initial quantity used for nanoparticle preparation) into the WSC component prior to fiber drawing. A three-dimensional nonwoven fibrous scaffold was constructed using needle-punching, in essence mechanically creating physical entanglements among the fibers. Prior to cell seeding experiments, the scaffold was sterilized by multiple washing steps in phosphate-buffered saline alternating with 70% ethanol and then lyophilized overnight. Heterogeneous nanoparticle-loaded scaffolds comprising 30% fibers encapsulating pEGFP-C1 (NP–GFP) and pVR1055-bFGF (NP–bFGF) plasmids, as well as blank scaffolds consisting solely of WSC and alginate fibers without nanoparticles, were prepared.

### Cell seeding

HEK293 and HDF cells were selected as model cell lines for cell seeding and transfection experiments. Cells were suspended in medium at a concentration of  $2.5 \times 10^6$ /ml and seeded by pipetting 200  $\mu$ l of cell suspension drop-wise onto a 75-mm<sup>3</sup> piece of dry scaffold ( $\sim$ 15  $\mu$ g DNA/piece) in a 24-well plate Transwell membrane (Costar). Scaffolds were transferred out of the Transwell into 1.5 ml/well of medium in wells of a 24-well plate after 1 day. Cell seeding efficiency was quantified by detaching and counting the cells remaining in the Transwell at that time and subtracting from the original number of cells seeded. The medium was changed every 3 days, and in the case of constructs containing bFGF-encoding plasmid nanoparticles, 1 ml of medium was sampled and frozen at  $-20^\circ\text{C}$  for later analysis of extracellular transgene protein concentration. Blank scaffolds were used as negative controls in all experiments. Scaffolds seeded with HEK293 cells were cultured in Eagle minimum essential medium supplemented with 1.5 g/L sodium bicarbonate, 0.1 mM nonessential amino acids, 1.0 mM sodium pyruvate, and 10% heat-inactivated horse serum. HDF-seeded scaffolds were incubated in Dulbecco's modified Eagle medium supplemented with 10% fetal bovine serum and 1% penicillin/streptomycin (Gibco, Carlsbad, CA, USA).

## Two-dimensional cell culture controls

Cells in two-dimensional plate culture were transfected with PEI–DNA nanoparticles to compare the long-term efficiency of one-time delivery of plasmids versus anticipated extended transfection from the three-dimensional scaffolds. Briefly, cells plated at 70% confluence were transfected with PEI–DNA nanoparticles containing bFGF-encoding plasmid for 4 h, after which the medium was changed. After 3 days, the medium was sampled and stored at  $-20^{\circ}\text{C}$ , and cells were transferred to 35-mm petri dishes and cultured for up to 6, 9, 12, 15, and 18 days, with medium sampling at these time points. A second two-dimensional control was performed by transfecting cells with pGFP complexed with LipofectAMINE reagent and analyzed with flow cytometry (FACScan) for GFP expression after 3 days.

The stability of bFGF in the culture medium was evaluated by incubating 200 pg/ml bFGF for 1 and 3 days and then measuring the concentration of growth factor remaining. This was compared against the background level in the medium without exogenous bFGF added.

## Analysis techniques

Single fibers as well as needle-punched scaffolds were dehydrated in a series of ethanol drying steps and then coated with 5 nm of chromium for observation under scanning electron microscopy (Leo FESEM). The viability of cells seeded on the scaffold was evaluated 21 days postseeding using the Live/Dead Viability/Cytotoxicity Kit (Molecular Probes, Eugene, OR, USA) based on the principle of enzymatic conversion of nonfluorescent calcein AM to fluorescent calcein (495/515 nm) by intracellular esterase and the binding of ethidium homodimer-1 to nucleic acids in cells with damaged membranes, resulting in enhancement of fluorescence (495/635 nm). To confirm the presence of nanoparticles, single fibers as well as scaffold samples were stained with Hoechst 33258 dye (Molecular Probes) and observed using a Nikon TE3000 Eclipse inverted microscope equipped with a UV filter (350/450 nm). NP–GFP cell-seeded scaffolds were cultured for up to 2 weeks and observed for cytosolic GFP expression using a Zeiss LSM 410 confocal microscope (543 nm) on day 12. A Hoechst counterstain was used in all scaffold samples to indicate the location of cell nuclei. Cells from NP–GFP scaffolds were trypsinized from the scaffold on day 12 and GFP expression was quantified using flow cytometry in a FACSCalibur. The wavelength of the detection bandpass filter was 530 nm; the gating was set above the level of the major cluster on the dot plot for the negative control (nontransfected cells) so as to exclude at least 99% of the data points. Extracellular bFGF content in medium collected from NP–bFGF scaffolds as well as two-dimensional controls was quantified using a DuoSet bFGF ELISA kit (BD Biosciences, Minneapolis, MN, USA) according to the manufacturer's instructions and normalized to the total number of cells that were attached to the scaffold 24 h post-cell seeding.

## Statistical analysis

Statistical significance was computed using the one-tailed Student *t* test. A significance level of  $P < 0.05$  is indicated by an asterisk in the figures.

## Acknowledgements

The authors thank Corrine Bright and Ruijiang Song, for creating the pVR1055-bFGF plasmid, and Evelyn Yim for insightful discussions. S. H. Lim acknowledges the Singapore Economic Development Board for an Exxon–Mobil scholarship. Funding support from the NIH (EB003447) is also acknowledged.

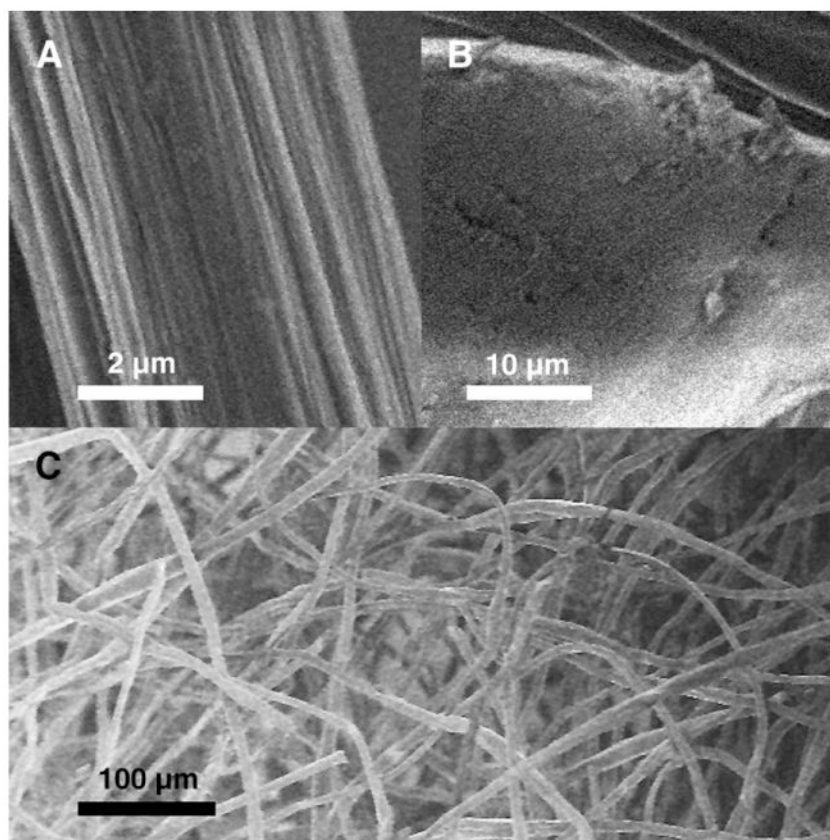
## References

1. Murphy WL, Mooney DJ. Controlled delivery of inductive proteins, plasmid DNA and cells from tissue engineering matrices. *J Periodontal Res* 1999;34:413–419. [PubMed: 10685370]

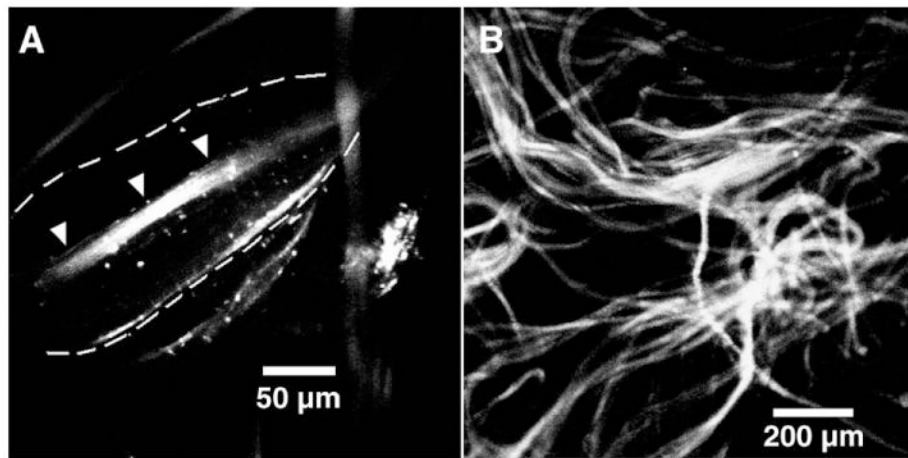


2. Jansen JA, et al. Growth factor-loaded scaffolds for bone engineering. *J Controlled Release* 2005;101:127–136.
3. Chew SY, Wen J, Yim EK, Leong KW. Sustained release of proteins from electrospun biodegradable fibers. *Biomacromolecules* 2005;6:2017–2024. [PubMed: 16004440]
4. Ziegler J, Mayr-Wohlfart U, Kessler S, Breitig D, Günther KP. Adsorption and release properties of growth factors from biodegradable implants. *J Biomed Mater Res* 2002;59:422–428. [PubMed: 11774299]
5. Wei G, Pettway GJ, McCauley LK, Ma PX. The release profiles and bioactivity of parathyroid hormone from poly(lactic-co-glycolic acid) microspheres. *Biomaterials* 2004;25:345–352. [PubMed: 14585722]
6. Lu L, Yaszemski MJ, Mikos AG. TGF-beta1 release from biodegradable polymer microparticles: its effects on marrow stromal osteoblast function. *J Bone Joint Surg Am* 2001;83-A:S82–91. [PubMed: 11314800]
7. Bonadio J, Smiley E, Patil P, Goldstein S. Localized, direct plasmid gene delivery *in vivo*: prolonged therapy results in reproducible tissue regeneration. *Nat Med* 1999;5:753–759. [PubMed: 10395319]
8. Jang JH, Rives CB, Shea LD. Plasmid delivery in vivo from porous tissue-engineering scaffolds: transgene expression and cellular transfection. *Mol Ther* 2005;12:475–483. [PubMed: 15950542]
9. Shea LD, Smiley E, Bonadio J, Mooney DJ. DNA delivery from polymer matrices for tissue engineering. *Nat Biotechnol* 1999;17:551–554. [PubMed: 10385318]
10. Huang YC, Simmons C, Kaigler D, Rice KG, Mooney DJ. Bone regeneration in a rat cranial defect with delivery of PEI-condensed plasmid DNA encoding for bone morphogenetic protein-4 (BMP-4). *Gene Ther* 2005;12:418–426. [PubMed: 15647766]
11. Wan AC, Yim EK, Liao IC, Le Visage C, Leong KW. Encapsulation of biologics in self-assembled fibers as biostructural units for tissue engineering. *J Biomed Mater Res A* 2004;71:586–595. [PubMed: 15499568]
12. Roy K, Mao HQ, Huang SK, Leong KW. Oral gene delivery with chitosan-DNA nanoparticles generates immunologic protection in a murine model of peanut allergy. *Nat Med* 1999;5:387–391. [PubMed: 10202926]
13. Mao H-Q, et al. Chitosan–DNA nanoparticles as gene carriers: synthesis, characterization and transfection efficiency. *J Controlled Release* 2001;70:399–421.
14. Zhang Y, Zhang M. Calcium phosphate/chitosan composite scaffolds for controlled in vitro antibiotic drug release. *J Biomed Mater Res* 2002;62:378–386. [PubMed: 12209923]
15. Chung TW, et al. Preparation of alginate/galactosylated chitosan scaffold for hepatocyte attachment. *Biomaterials* 2002;23:2827–2834. [PubMed: 12069321]
16. Howling GI, et al. The effect of chitin and chitosan on the proliferation of human skin fibroblasts and keratinocytes in vitro. *Biomaterials* 2001;22:2959–2966. [PubMed: 11575470]
17. Genes NG, Rowley JA, Mooney DJ, Bonassar LJ. Effect of substrate mechanics on chondrocyte adhesion to modified alginate surfaces. *Arch Biochem Biophys* 2004;422:161–167. [PubMed: 14759603]
18. Kamiya N, Klibanov AM. Controlling the rate of protein release from polyelectrolyte complexes. *Biotechnol Bioeng* 2003;82:590–594. [PubMed: 12652482]
19. Rowley JA, Mooney DJ. Alginate type and RGD density control myoblast phenotype. *J Biomed Mater Res* 2002;60:217–223. [PubMed: 11857427]
20. Yan XL, Khor E, Lim LY. Chitosan–alginate films prepared with chitosans of different molecular weights. *J Biomed Mater Res* 2001;58:358–365. [PubMed: 11410893]
21. Haque T, et al. Investigation of a new microcapsule membrane combining alginate, chitosan, polyethylene glycol and poly-l-lysine for cell transplantation applications. *Int J Artif Organs* 2005;28:631–637. [PubMed: 16015573]
22. Simsek-Ege FA, Bond GM, Stringer J. Polyelectrolyte complex formation between alginate and chitosan as a function of pH. *J Appl Polym Sci* 2003;88:346–351.
23. Takahashi Y, Hachisu M, Ohkawa K, Yamamoto H. Water-soluble polypeptides at aqueous interface produce extensible silk-like fiber. *Macromol Rapid Commun* 2002;23:540–543.

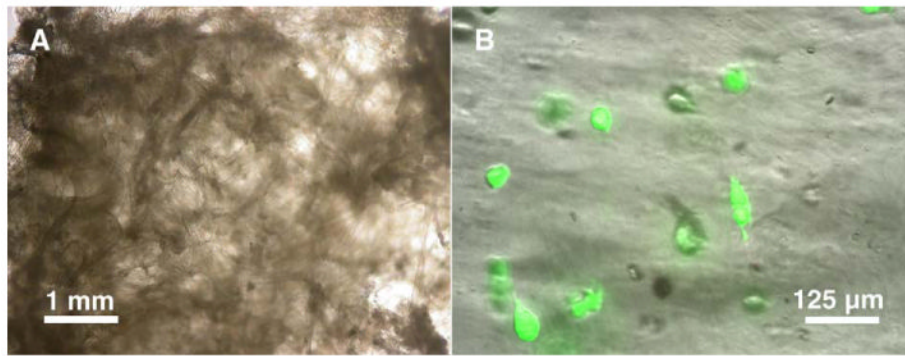
24. Ohkawa K, Takahashi Y, Yamada KM, Yamamoto H. Polyion complex fiber and capsule formed by self-assembly of chitosan and poly(L-glutamic acid) at solution interfaces. *Macromol Mater Eng* 2001;286:168–175.
25. Liao IC, Wan AC, Yim EK, Leong KW. Controlled release from fibers of polyelectrolyte complexes. *J Controlled Release* 2005;104:347–358.
26. Goula D, et al. Polyethylenimine-based intravenous delivery of transgenes to mouse lung. *Gene Ther* 1998;5:1291–1295. [PubMed: 9930332]
27. Subramanian S, Srienc F. Quantitative analysis of transient gene expression in mammalian cells using the green fluorescent protein. *J Biotechnol* 1996;49:137–151. [PubMed: 8879169]
28. Steiling H, Werner S. Fibroblast growth factors: key players in epithelial morphogenesis, repair and cytoprotection. *Curr Opin Biotechnol* 2003;14:533–537. [PubMed: 14580585]
29. Nimni ME. Polypeptide growth factors: targeted delivery systems. *Biomaterials* 1997;18:1201–1225. [PubMed: 9300556]
30. Luo D, Saltzmann WM. Enhancement of transfection by physical concentration of DNA at the cell surface. *Nat Biotechnol* 2000;18:893–895. [PubMed: 10932162]
31. Xie Y, Yang ST, Kniss DA. Three-dimensional cell-scaffold constructs promote efficient gene transfection: implications for cell-based gene therapy. *Tissue Eng* 2001;7:585–598. [PubMed: 11694192]
32. Cukierman E, Pankov R, Stevens DR, Yamada KM. Taking cell–matrix adhesions to the third dimension. *Science* 2001;294:1708–1712. [PubMed: 11721053]
33. Brunner S, Sauer T, Carotta S, Saltik M, Wagner E. Cell cycle dependence of gene transfer by lipoplex, polyplex and recombinant adenovirus. *Gene Ther* 2000;7:401–407. [PubMed: 10694822]
34. Huang YC, Connell M, Park Y, Mooney DJ, Rice KG. Fabrication and in vitro testing of polymeric delivery system for condensed DNA. *J Biomed Mater Res* 2003;67A:1384–1392.
35. Huang YC, Riddle K, Rice KG, Mooney DJ. Long-term in vivo gene expression via delivery of PEI–DNA condensates from porous polymer scaffolds. *Hum Gene Ther* 2005;16:609–617. [PubMed: 15916485]
36. Sannan T, Kurita K, Iwakura Y. Studies on chitin. 1. Solubility change by alkaline treatment and film casting. *Makromol Chem –Macromol Chem Phys* 1975;176:1191–1195.
37. Tan SC, Khor E, Tan TK, Wong SM. The degree of deacetylation of chitosan: advocating the first derivative UV-spectrophotometry method of determination. *Talanta* 1998;45:713–719.
38. Boussif O, et al. A versatile vector for gene and oligonucleotide transfer into cells in culture and *in vivo*: polyethylenimine. *Proc Natl Acad Sci USA* 1995;92:7297–7301. [PubMed: 7638184]



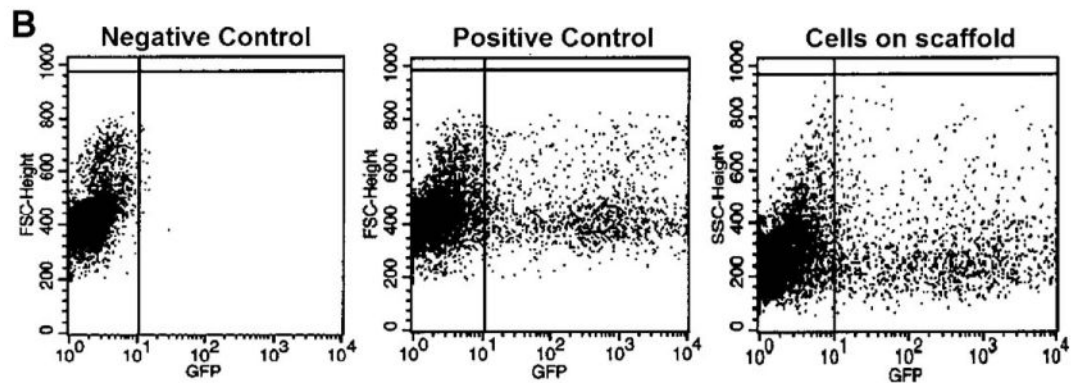
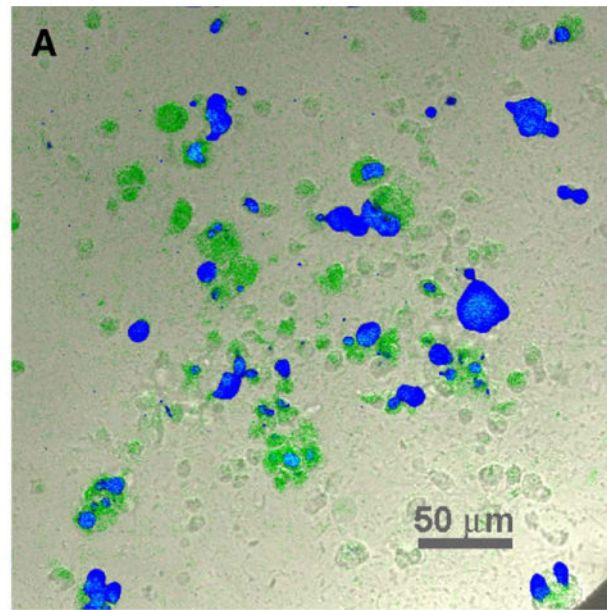
**FIG. 1.** Scanning electron micrographs of the single PEC fiber as well as a needle-punched nonwoven fibrous scaffold. (A) Core fiber segment with striations on the surface. (B) Bead region with a smoothed surface. (C) Macroscopic view of nonwoven fibrous scaffold possessing high porosity.



**FIG. 2.** Confocal images of fibers and scaffold encapsulated with PEI–DNA nanoparticles. PEI–DNA nanoparticles encapsulated within the fibers were fluorescently stained with Hoechst 33258 dye. (A) Phase microscopy of the bead region of a single fiber shows that nonaggregated nanoparticles were evenly but sparsely dispersed within the bead (outlined by dotted lines) but at higher density in the core fiber segment (indicated by arrowheads). (B) Fibers containing nanoparticles were mixed with blank fibers in a 3:7 ratio and a heterogeneous nonwoven scaffold was formed by needle-punching.

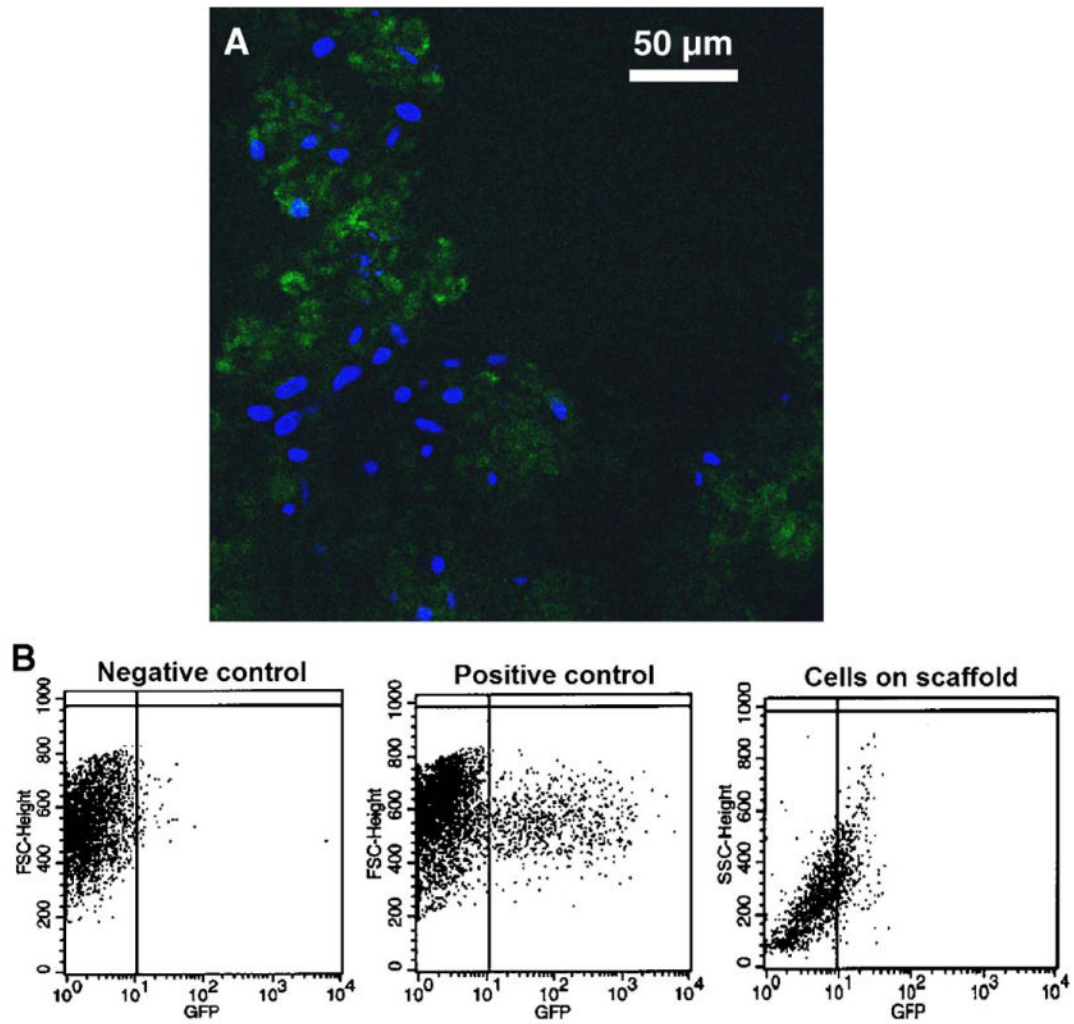


**FIG. 3.** Images of blank and cell-seeded scaffolds. (A) When wetted, scaffolds swelled visibly and decreased in opacity but still retained their fibrous morphology, with most of the swelling confined to the bead regions. (B) Cells seeded on the scaffold remained viable even after 3 weeks of culture, although some cells had detached from the fibers, resulting in decreased cell seeding density.



**FIG. 4.**

Transgene expression of HEK293 cells seeded on fibrous scaffolds loaded with PEI-DNA nanoparticles. (A) Samples of the cell-scaffold constructs were viewed using confocal microscopy at 12 days postseeding, at which active expression of cytoplasmic GFP within distinct single cells was still observed. Samples were cross-stained with Hoechst 33258 to indicate the locations of cell nuclei. The image is a pseudo-color RGB overlay. (B) Flow cytometry indicates that the proportion of GFP-positive cells compared favorably with the positive control. (For interpretation of the references to colour in this figure legend, the reader is referred to the web version of this article.)

**FIG. 5.**

Transgene expression of human dermal fibroblasts seeded on fibrous scaffolds loaded with PEI–DNA nanoparticles containing GFP-encoding plasmid. (A) At 12 days postseeding, large numbers of fibroblasts were actively expressing GFP; fibroblasts also exhibited increased tendency to aggregate compared with HEK293 cells. (B) Flow cytometry data indicates that the intensity of GFP expression in fibroblasts was not as high as that of the positive control, but nonetheless present.

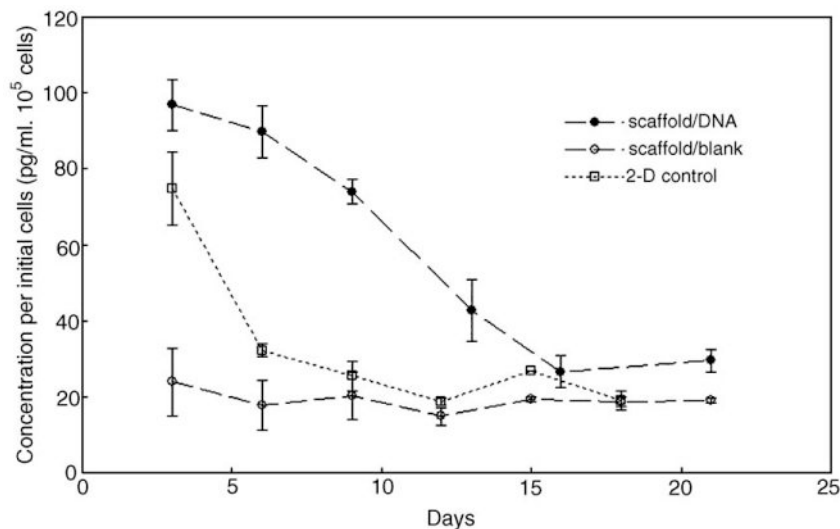


**FIG. 6.** Transgene expression of human dermal fibroblasts seeded on fibrous scaffolds loaded with PEI–DNA nanoparticles containing bFGF-encoding plasmid. Cell medium was sampled at frequent intervals and assayed for extracellular bFGF concentration over a period of 3 weeks. Results were normalized to the initial number of cells seeded on the scaffold. (Solid circles, scaffold with encapsulated nanoparticles; open circles, cells seeded on blank scaffold with no encapsulated nanoparticles; open squares, two-dimensional cell control—cells seeded on TCPS were transfected at day 0 and bFGF production was monitored thereafter).



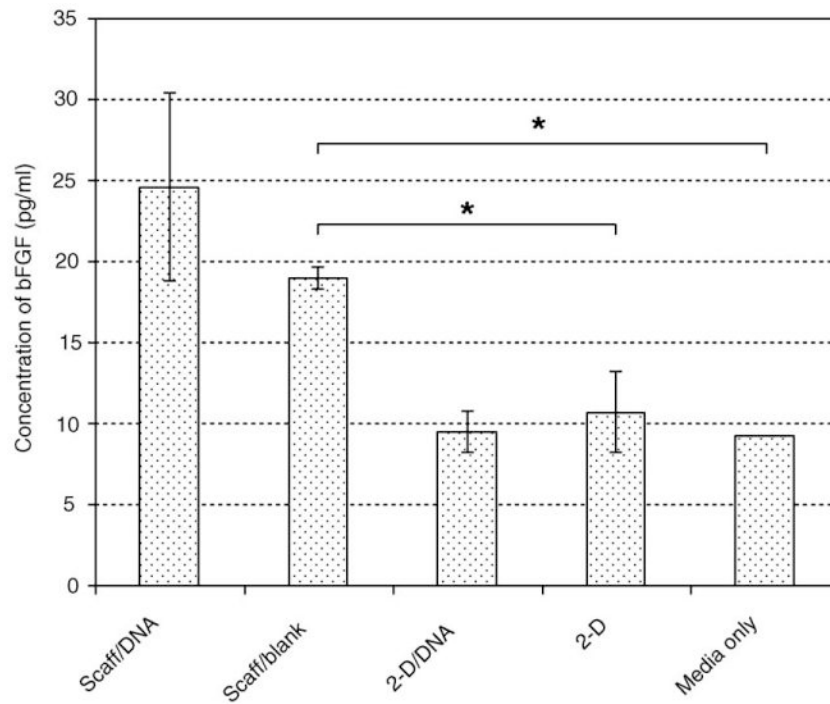


**FIG. 7.** End-point concentrations of extracellular bFGF, not normalized to initial cell number. (Scaff/DNA, fibrous scaffold with encapsulated DNA nanoparticles; Scaff/blank, fibrous scaffold without encapsulated DNA nanoparticles; 2-D/DNA, bolus transfection of cells seeded on TCPS; 2-D, nontransfected cells on TCPS.) Cells seeded on three-dimensional fibrous scaffolds without nanoparticles nonetheless produced a low level of endogenous bFGF, which was not detected in cells grown on TCPS (detected levels were the same as cell medium alone).